Integrative Biology

Accepted Manuscript

ROYAL SOCIETY OF CHEMISTRY

www.rsc.org/ibiology

Insight statement

There is a growing body of work dedicated to producing acellular lung scaffolds for use in regenerative medicine by decellularizing donor lungs of various species. In this work, we propose a new systematic decellularization technique that can effectively remove donor DNA, yet retain critical structural, adhesive, and supportive proteins such as collagen, elastin, laminin, and fibronectin, and polysaccharides such as s-GAGs in lung tissue. As a result of this matrix retention, the resulting mechanical properties of the acellular tissues are remarkably similar to native lung. Taken together, these results suggest that the proposed decellularization protocol provides a time efficient and reproducible method to create acelluar scaffolds for use in tissue engineering. The primary benefits of a nearly intact tissue matrix will likely become even more apparent in future, longer-term studies.

Introduction

Respiratory disease has become one of the leading causes of death in the United States and throughout the world. In the US alone, over 24 million adults have evidence of impaired lung function, resulting in a considerable physical and financial burden [1]. Currently, lung transplantation is the only definitive therapy for patients with end-stage lung disease; however, severe organ shortage prevents transplantation from being a practical solution for the majority of these patients. The current donor lung shortage is also exacerbated by the fragility of the organ. Lung tissues are easily damaged and often compromised during the process of procurement and transplantation. In addition to these limitations, patients are required to be on life-long immunosuppressive regimens after lung transplant, resulting in severe reduction in quality of life and an increased vulnerability to pulmonary infections [2]. The creation of a sterile, autologously-cell sourced bioengineered lung would decrease the morbidity associated with immunosuppression and the donor organ shortage, and it would also provide a means to tailor lung replacements for patients with a wide range of physiological needs.

There is a growing body of work that is dedicated to the creation of acellular scaffolds fabricated by decellularizing donor lungs [3-12]. Porcine lung tissue has gained popularity for use in decellularization studies, as both a model of human tissue and also a potential scaffold for transplantation [13-17]. The extracellular matrix (ECM) that remains after lung decellularization is not an inert material, but rather a complex milieu of physical signals that encodes a 'biochemical and mechanical language' for resident cells. ECM-cell interactions govern cell viability, signaling pathways, proliferation, and

differentiation [18-20]. Therefore, even seemingly minute changes in these matrix cues may induce positive outcomes such as cell engraftment and directed cell differentiation, or negative outcomes such as reduced cell attachment, cell death, inflammation, and cell-driven fibrotic matrix remodeling. In fact, ECM breakdown is considered to be a primary contributor to the progression of several lung pathologies [21]. Therefore, we hypothesize that to produce a scaffold capable of supporting the growth of diverse populations of pulmonary cells, it is imperative that the acellular lung tissue maintain as much of the original (healthy) matrix architecture and protein components as possible.

Detergents that are commonly used in the decellularization process include Triton X-100, sodium dodecyl sulfate (SDS), sodium deoxycholate (SDC), and 3-[(3-cholamindopropyl)dimethylammonio]-1-propanesulfonate (CHAPS). These detergents solubilize cell membranes, disengage cytoskeletal proteins from cells, and detach DNA and DNA remnants from proteins [22]. Successful decellularization would require the removal of cell membrane epitopes, damage-associated molecular pattern (DAMP) molecules, and DNA remnants from the scaffold, as these components are known to induce inflammatory reactions [21, 23-25]. In addition, as detergent efficiency is cell-type dependent [26, 27] and there are multiple resident cell types in the lung, an ideal decellularization protocol would likely utilize a combination of detergents.

Decellularization is a delicate balance between effective cell removal and preservation of critical matrix components. As detergents remove cellular debris, these solutions simultaneously extract and damage components of the ECM that are essential to lung function and cell adhesion, including various glycoproteins and proteoglycans [28]. To date, an analysis of various decellularization protocols utilized on porcine lungs has

demonstrated matrix deterioration ranging in severity. Reported matrix damage includes loss of collagen, [15, 16] elastin, [13, 15, 16], laminins, [16] fibronectin, [14, 16] and sulfated glycosaminoglycans (GAGs) [4, 13]. The functional consequences of specific protein removal can range from impaired cell engraftment due the loss of fibronectin [29] to complete loss of tissue strength from loss of collagen type I [30]. The development of a decellularization protocol that is designed to minimize matrix damage would provide an important step toward the creation of a viable scaffold for use in tissue engineering.

The work presented herein describes an improved decellularization method for porcine lungs that utilizes mild detergents at low concentrations, as well as reduced fluid volumes and processing times as compared to some previously reported protocols. This method utilizes neutral pHs (all solutions between pH 7-8) to promote the retention of key matrix proteins and tissue architecture. The entire protocol can be completed for a set of adult-sized lungs in approximately 24 hours. In addition, we extend this protocol for use in individual lobes, presenting a protocol that is scaled by tissue mass in order to provide a more generalizable and reproducible method that could apply to organs from different species and donor ages. Characterization of the decellularized porcine lung tissues demonstrates retention of microscopic and macroscopic architecture of the pleura, airways, and vasculature, as well as preservation of tissue mechanics.

Results

Assessment of decellularization protocol on whole lungs and individual lobes

In all cases, the described decellularization protocol consistently produced a translucent

white scaffold with no gross morphological differences between tissue samples (Fig. 1A and B). As evidenced by H&E images, no intact nuclei or DNA smears were visible in the alveolar septae or vasculature after treatment, yet the overall microarchitecture of the lung was preserved (Fig. 1C-F). The resultant decellularization protocol was deemed to be effective for both whole tissues and individual lobes. Therefore, subsequent characterization was performed on decellularized accessory lobes. Whole lungs from Yorkshire pigs ranged from 200-300 grams total weight (Fig. 1A), whereas accessory lobes ranged between 15-21 grams (Fig. 1B). The decellularized tissue retained microstructure similar to native tissue, with intact alveolar septae, vasculature, and upper airways (Figs. 1E and F; and 2A and F). The decellularized matrix also retained the majority of key structural proteins by immunohistochemistry, including collagen type I and elastin fibers throughout the entirety of the lung tissues (Figs. 2B and G; and 2C and H). It was evident that a substantial amount of fibronectin remained present throughout the matrix (Fig. 2D and I).

In addition, immunostaining showed that two prevalent forms of collagen in the lung (collagens type I and IV) were homogenously distributed in both the central and peripheral regions, indicating the preservation of both fibrillar and basement membrane collagens (Figs. 2B and G; and 3A and D). Elastin, the matrix component responsible for the elastic recoil of lung tissue, was also preserved in both the vasculature and the lung parenchymal regions (Fig. 2C and H; and 3B and E). Laminins, a class of proteins that plays a key role in epithelial cell-matrix adhesion and cell motility was also somewhat preserved (Fig. 3C and F). Taken together, these data suggest that under this decellularization protocol, the resulting acellular scaffold is very similar to native tissue

with respect to collagens, and retains a substantial amount of other key matrix proteins including elastin, fibronectin, and laminins.

Quantitative analyses of lung matrix:

The carbazole assay revealed a significant loss (49% reduction, Fig. 4A) of total GAGs in the decellularized matrix as compared to native (n=6, 4 respectively; $p = 0.03$). This result was confirmed by the observed depletion of GAGs in the Toluidine Blue stain (Figs. 2E and J). Given that a large percentage of GAGs are intracellular [31], a significant loss of GAGs after decellularization is to be expected. When measuring sulfated GAGs (s-GAGs), the acellular scaffolds did not undergo significant s-GAG depletion as demonstrated by only 15% loss compared to native (n=12, 15 respectively; Fig. 4B). Therefore, the majority of GAGs removed during decellularization with this method are unsulfated GAGs (Fig. 4C).

There was preservation of total collagen content after decellularization (Fig. 4D), as evidenced by a lack of statistical difference between native and acellular tissue by hydroxyproline assay (n=6, 12 respectively, $p = 0.35$). The efficiency of decellularization was assessed by measuring residual DNA and by immunoblotting for cytoskeletal proteins. The decellularized lung demonstrated a 96% reduction in DNA as compared to native tissue (0.15 μg/mg vs. 3.7 μg/mg wet tissue, respectively). This amount of DNA was significantly lower in decellularized tissue compared to native lung (n=12, 15 respectively; $p < 0.001$), and also had no evidence of the cytoskeletal protein vimentin as detectable by immunoblotting (Figs. 4E and F). These data are supported by the complete lack of intact nuclear material as evidenced by H&E (Fig. 1E and F) and DAPI staining (Fig. 3D-F) and by the minimal presence of residual cellular debris.

Therefore, the protocol utilized herein produces an acellular scaffold with minimal donor DNA and cytoskeletal components.

Comparison of current method to alternative decellularization protocols

Pig lobes were decellularized using two commonly utilized decellularization protocols and compared to our proposed decellularization method. Briefly, the "Triton X-100/SDC II (high concentration)" consists of a 0.1% Triton X-100 and 2% SDC solution installation and perfusion, followed by a DNAse rinse. The "SDS" method consisted primarily of perfusing 0.5% SDS via the vasculature 3 days. No DNAse was used in this protocol.

Matrix retention and effective decellularization were determined by examining gross morphological microarchitecture, DNA and s-GAG content, and mechanical properties of the tissue (Fig. 5A-E). The overall architecture of the lung was well-preserved in all decellularized groups (Fig. 5A). In terms of effective DNA removal, no intact nuclei were visible in the alveolar septae or vasculature in any of the decellularized tissues, although there were detectable DNA smears in SDS-treated tissue (Fig 5, 6). In addition, all decellularized tissues had statistically lower DNA as compared to native (Fig. 5B and E), although tissues decellularized via SDS retained 3-5 fold more DNA than other decellularization regimes. There was no statistical difference in DNA content between tissues decellularized with the method proposed in this work ("current"), and tissues decellularized with higher concentrations of Triton X-100/SDC. In terms of matrix retention, s-GAG content was the highest in the current method and nearly undetectable

in tissues decellularized with higher concentrations of Triton X-100/SDC (Fig. 5C and E).

Results from mechanical testing of the native and decellularized tissues are shown in Figure 5D. For an excellent review of pulmonary matrix mechanics please refer to reviews by Suki and colleagues. [32, 33]. At deformations within typical tidal volumes (i.e., 1-10% strain) [34-36], all decellularized tissue closely resembled native lung (Fig. 5D and E). Specifically, at lower strain levels (i.e. 5% strain), all decellularized tissue had Young's moduli that did not differ significantly from native. However, under large deformations, only tissues decellularized with the protocol proposed in this work ("current") mimics native mechanical characteristics. For example, when examining stress-strain curves at higher strain levels (i.e. 30% strain), tissues decellularized via the proposed current method were not significantly different than native tissue (67.4 kPa versus 77.7 kPa, respectively, $p = 0.08$). Tissues decellularized using the previously reported Triton X-100/SDC protocol were significantly softer than native tissues (54.3 versus 77.7 kPa, respectively, $p = 0.008$). It should be noted, however, that all acellular lung scaffolds decellularized using Triton X-100/SDC combinations (i.e., "current" and "Triton/SDC") had an enhanced 'toe region' when compared to native lung (Fig. 5D). Tissues decellularized with SDS were brittle and significantly stiffer than native lung at higher strain levels (143.5 versus 77.7 kPa, respectively, $p = 0.0008$), and these tissues consistently failed under lower deformations (~30-40%).

Recellularization and slice culture

To determine which method of decellularization (Triton/SDC I, Triton/SDC II, or SDS)

yielded acellular tissue adequate for cell seeding, 300 μm sections of lung tissue were reseeded with A549 cells and examined for cell engraftment and health (Fig 6). Acellular tissues procured using the Triton/SDS I method enabled homogeneous epithelial cell engraftment in both the large airways and the alveolar regions of the tissue. Acellular tissues procured via the Triton/SDC II protocol did not promote cell engraftment throughout the tissue, rather cells adhered to the perimeter of the tissue only demonstrating preference to the tissue culture plastic over the acellular tissue. Tissues produced using the SDS protocol engrafted throughout the tissue, although the tissue was much more sparse than the Triton X/SDC I protocol. Therefore, the resulting acellular tissue is capable of providing a suitable scaffold for cell growth, and acellular tissue decellularized using the Triton X/SDC I method demomstrated superior egraftment.

Discussion

Creating acellular lung scaffolds from large animal or human sources provides a very difficult set of challenges: the prevention of clot formation during tissue acquisition, handling of large volumes of detergents during processing, size and biological variability between donors, and the need for complete removal of donor cell material in order to limit recipient immune response. Blood clearance and clot prevention prior to processing are critical for two reasons: 1) blood exposure to detergents can result in protease activation and ECM breakdown, [22, 37] and 2) clot formation will prevent adequate perfusion of detergents through the vasculature, resulting in insufficient decellularization. In addition, goals for effective decellularization include retention of critical matrix components to ensure mechanical integrity and biological activity, conservation of

183 microvascular lumens that are free from occlusion with cellular debris, and the
184 preservation of relatively soluble glycoproteins and proteoglycans that mediate cell
185 adhesion. Although the pigs were pretreated with high doses of heparin (500 U/kg), we
186 utilized heparin (100 U/ml) during the clearance and washing steps prior to
187 decellularization. Lastly, since all lungs are non-sterile at time of procurement, bacterial
188 and fungal eradication for subsequent cell culture must be achieved, either during the
189 decellularization process, or with a discrete sterilization step.

190 To date, the majority of decellularization protocols were developed with the principal
191 design criteria of producing an ECM framework having minimal donor DNA. Therefore,
192 the goal was not necessarily to retain matrix composition, but rather to create a platform
193 with the general architectural features of a lung and little detectible cell debris. Current
194 methods of porcine lung decellularization result in severe matrix damage, with reports of
195 up to 50% collagen loss [15], 40-64% elastin loss [13, 15], 80% loss of sulfated GAGs
196 [13] and general loss (i.e., not quantified) of collagen type IV [16], laminin [16], and
197 fibronectin [14, 16]. Each of these previously described procedures results in the
198 destruction or removal of least one critical matrix protein. Therefore, although these
199 methods provide an excellent model of matrix degradation as seen in aging or lung
200 disease [6, 38] and have contributed to our fundamental understanding of cell-matrix
201 interactions, these decellularization protocols render a depleted scaffold and may not be
202 optimized for long-term cell culture.

203 By determining the minimal amount of detergent required for cell removal, using
204 physiological levels of pressure, and maintaining neutral pHs of our solutions, we were
205 able to provide an acellular scaffold with unprecedented levels of matrix retention.

Specifically, we enabled retention of collagen types I and IV, sulfated GAGs, and laminin in the acellular tissue. We also observed a marked retention of elastin and fibronectin in the airways and vasculature. Reports in literature of what is described as an "acellular lung matrix" ranges from ~75-98% donor DNA removal [3, 4, 10, 13, 15, 39]. Despite the mild decellularization conditions reported here, we observed similar if not greater levels of DNA removal when compared to protocols with much harsher regimens (96%, Fig. 5B). There are several reasons for the effectiveness of this protocol: highly effective blood clearing, processing fresh as opposed to frozen tissues, multiple washing steps, the use of DNAase, avoiding detergent precipitation (e.g., removal of salt from higher SDC concentrations), and also the ramping of detergent concentrations to assist in the removal of DNA in a gentle manner. In terms of the implications of the residual donor DNA, the percent reduction is greater than previously reported in tissues that incited minimal host immungenetic response [40]. Further, it is possible to assist in donor DNA removal by washing the tissue with serum as reported previously [41].

With respect to GAG retention, we found retention of 51% of total GAGs, as evidenced by both histology and direct measurements (carbazole assay; Fig 4A) and no significant loss of sGAGs (5C, E). Although other groups have also reported similar levels of sulfated GAG retention [15], it is surprising that sulfated GAGs would be retained so significantly in the matrix given that sulfated heparan sulfate is highly abundant on pulmonary endothelium (removed in our process) [42]. Measuring partially degraded material post decellularization could be contributing to these discrepancies; to address this concern, decellularization effects on matrix composition should be assessed using multiple assays, if and when they are available.

In previous studies, our group and others utilized CHAPS at pH 12 as a primary decellularization detergent. However, the use of a harsher detergent at a high pH resulted in a significant loss of elastin (~60%), proteoglycans (~95%), and the majority of fibronectin [4, 13, 30]. The resulting lung matrix also induced a strong inflammatory response in rats that were implanted with decellularized tissue, although this response appeared to be diminished when tissues were decellularized at neutral pHs [43]. Although acidic or basic detergents have been used previously to assist in the decellularization process, these non-physiological pH conditions can also catalyze the hydrolytic degradation of the lung matrix [10, 20, 44]. These conditions can result in the complete elimination of matrix-embedded growth factors, degradation of structural proteins such as collagen fibers, and significant alteration of the mechanical properties of the matrix [45, 46]. Another commonly used detergent, SDS, has also been shown to cause damage to tissue architecture, remove collagen, and eliminate GAGs [13, 15, 16, 30]. Although we did not investigate the retention or removal of growth factors in this study, our findings support the growing discussion of the negative impact of SDS-based decellularization on matrix retention and cell engraftment in porcine lungs (Fig. 5) [13, 15].

Triton X-100 is not only a detergent but also a disinfectant that can be utilized to combat lung-related infection. Triton X-100 has been shown to remove biofilms [47], inactivate H1N1 [48], and lower the resistance of methicillin-resistant staphylococcus aureus (MRSA) to antibiotics at concentrations as low as 0.02% [49]. Currently, peracetic acid and/or ethanol is typically utilized to sterilize lung tissue [6, 9, 14], though there is some evidence that these treatments can result in growth factor removal and

damage or cross-linking to the matrix [50, 51].

Although other research groups have developed decellularization protocols using Triton X-100/SDC combinations, this protocol utilizes SDC concentrations that are 20 times lower than those previously reported (0.01-0.1%, as compared to 2-4%) [6, 10, 13-15, 17]. Low concentrations of SDC are key for the success of this protocol: SDC at 2% or greater is reported to deplete collagen, GAGs, and elastin content [10, 13, 15]. In some reports, GAG loss was at 86% loss or greater relative to native controls [10]. In this work, the impact of this depletion is event in significantly reduced s-GAG content (Fig. 5), and poor cell engraftment (Fig. 6). Interestingly, despite this 98% loss in s-GAG content, the mechanical alterations in mechanical properties of the tissue are only apparent at high deformations (Fig. 5E). Also surprisingly, despite a large ECM depletion seen in "Triton/SDC II", there is no substantial decrease in DNA levels (relative to our proposed protocol) in tissues decelled with higher SDS levels. It should be noted that although we do utilize Triton-X at a higher concentration than previously reported (0.5% versus 0.1%) [10, 17], this application is during a final step of the protocol subsequent to the decellularization steps (clearance and SDC application) and used during a rinse step (refer to Supplemental Figure 2). Triton-X during this step is primarily used as a surfactant in the removal of cell debris rather than as a detergent.

In addition to lower concentrations of detergents, our total decellularization protocol requires less than 24 hours of 'active' decellularization time. Previous reports of lung decellularization often require several days to weeks for proper cell removal [6, 15, 16]. The volumes of detergents can be tightly controlled, since decellularization is standardized by initial tissue weight. Previous reports either determine the extent of

decellularization by gross observation (aka “tissue whiteness”), or by using fixed reagent volumes to decellularize tissue [6, 14, 15].

In terms of the tissue integrity post decellularization, acellular tissue had a Young’s modulus that resembled native within physiological deformation ranges (i.e., 5-10% strain [52]). With respect to the mechanical analysis, the decellularized tissue did, however, have an extended ‘toe region’ (i.e. non-linear portion of the loading curve that precedes the linear portion of the curve). It is likely that these alterations in the tissue mechanics are due to the observed GAG loss in the tissue. GAGs contribute to the viscous component of tissue viscoelasticity by sequestering water [53], and also provide the lubricating film between adjacent fibers and reduce mechanical friction during higher states of deformation (i.e. levels of strain that typically rely on collagen load bearing). Chondroitin sulfate, for example, is attached to decorin and aides in collagen organization, and the removal or disruption of chondroitin has been shown to result in the disruption of the collagen fibrils, creating mechanical friction. Hence, partial depletion of GAGs may be contributing to changes in viscous behavior in the toe region of the stress-strain curves.

Conclusions

This study describes a reproducible decellularization protocol that can be utilized on a variety of tissue sizes. The entire protocol can be accomplished in approximately 24 hours, a duration that makes tissue processing feasible for many applications. The resulting matrix is acellular, yet retains critical structural, adhesive, and supportive proteins such as collagen, elastin, laminin, and fibronectin, and polysaccharides such as s-GAGs. Taken together, these results suggest that the proposed decellularization protocol

provides a time efficient and reproducible method to create acelluar scaffolds for use in tissue engineering. The primary benefits of a nearly intact tissue matrix will likely become even more apparent in future, longer-term studies.

Materials and Methods

Cell culture

Human A549 cells (a type II epithelial-like cell line) were cultured and expanded on tissue culture plastic at 37 °C and 5% CO2. A549s were cultured in Dulbecco's modified eagle medium (DMEM) supplemented with 10% fetal bovine serum (Hyclone) and 1% penicillin and 100 ug/ml streptomycin (Corning).

Tissue Procurement and harvest of organs

All animal experimental work was performed with approval from the Yale University Institutional Animal Care and Use Committee. All animal care complied with the Guide for the Care and Use of Laboratory Animals. Six, 20-25 kg Yorkshire pigs were pretreated intravenously with 500U/kg heparin to prevent intravascular clotting in the lung tissue after procurement. Pigs were subsequently euthanized via intraperitoneal injection of sodium pentobarbital (Sigma, 150 mg/kg). Immediately after euthanasia, the abdomen was entered via a transverse incision just below the costal margin. The diaphragm was punctured, and the rib cage was cut to reveal the lungs. The heart, lungs and trachea were dissected free from surrounding muscles and connective tissue and removed *en bloc*. The thymus was removed and care was taken not to disrupt the esophagus to minimize tissue damage and contamination during dissection. Whole lungs were either processed immediately (trachea and pulmonary artery cannulated) or the

accessory lobe was dissected from the whole lung, and the lobar bronchus and artery were cannulated.

The accessory lobe is the smallest of the seven lobes in the pig lung, and makes for a convenient model system for decellularization studies. The accessory lobe has easily accessible arterial and bronchial conduits (requiring one cannulation for vascular, and one for airway infusion), is isolated from other lobes, and can be dissected away from the lungs while maintaining an intact pleura [54, 55].

Decellularization Overview

In order to build a 'universal protocol' that would normalize for tissue size, we developed a decellularization regimen that operates on a volume of reagent/gram wet weight tissue basis (Table 1). Prior to decellularization, we first ensured proper blood clearance from the vasculature. Heparin has a very short biologic half-life [56], therefore additional heparin was administered during the decellularization processes to facilitate clearance of intra-vascular blood. For all blood and debris clearance and decellularization steps, the tissues were either perfused using a gravity feed at 22 mm Hg pressure via the vasculature (pulmonary artery (PA) for whole lungs, or artery for accessory lobe), or gently flushed manually via the airway (trachea for whole lungs, bronchus for accessory lobe).

Cannulation and Bioreactor Assembly

Cannulation and bioreactor assembly were based on Petersen et al [57]. Detailed figures depicting lung cannulation and the bioreactor design and assembly for both decellularization and culture are provided in Supplemental Figure 1. All fittings were

purchased from Cole-Parmer, and were sterilized prior to the decellularization process. Step 1: the airways and vasculature were cannulated using straight barbed connectors on a sterile medical instrument tray in a biosafety cabinet (BSC). Step 2: the fittings were directly sutured into the tissue and linked to a Y-splitter via a short segment of sterile tubing. Step 3: the Y-splitter attached to the vascular cannula was connected to a luer-lock fitting. This fitting was attached to the bioreactor's perfusion tubing for decellularization. Step 4: a one-way valve was connected to the segment of the Y-splitters that were not attached to the straight barbed connector, and allowed for air removal prior to fluid perfusion. Orientation of the valve was such that fluid could be drawn up into the tubing (in the opposite direction as perfusion) to remove air from the line, yet permitted fluid to flow into the lung during organ perfusion[5].

The bioreactor apparatus consisted of a custom-built large cylindrical glass reservoir, sealed from the external environment by a threaded plastic gasket and silicon cap (Supplemental Fig. 1B). The cap was equipped with segments of tubing that permitted sterile gas exchange via air filters, fluid removal and addition by a syringe port, and vasculature perfusion. The base of the cylindrical glass reservoir contained a two-way stopcock drain and the side of the chamber contained four threaded ports for additional fluid removal. All components of the apparatus were sterilized prior to assembly of the bioreactor. Refer to Supplemental Table 1 for detailed information regarding bioreactor components.

Organ Decontamination, Blood Clearance, and Decellularization

Refer to Table 1 for detailed decellularization protocol information regarding the fluids utilized and the volume, pH, temperature, and route of administration of each fluid.

365 All fluids were filter-sterilized inside the BSC prior to use. Immediately following en
366 bloc lung harvest, the airways of the tissue were inflated with PBS containing antibiotics
367 (10% penicillin/streptomycin, 4% amphotericin B, 2% gentamicin) to decrease survival
368 of colonizing organisms in the lung tissue. Following cannulation of the trachea and
369 vasculature, the vascular cannula was connected to the bioreactor cap using luer-lock
370 fittings. Subsequently, the lung was mounted within the bioreactor apparatus for
371 decellularization (Fig. 1B). The pulmonary view was not cannulated; it was left
372 uncannulated such that it could freely perfuse in one directly via gravity. The fluid simply
373 exited the lung's vasculature by way of the pulmonary vein into the bioreactor.

374 Aside from the initial antibiotic treatment (i.e. step 1a in Table 1) and endonuclease
375 (Benzonase, Sigma) application to the airway (i.e. steps 5b.1 and 5b.2 in Table 1), all
376 decellularization steps occurred through the vasculature via gravity perfusion at 22 mm
377 Hg. The tracheal cannula floated freely within the assembly during all steps except 5b.1
378 and 5b.2, when the lung was transiently removed from the bioreactor assembly for the
379 manual application of fluids (i.e. Benzonase and Benzonase buffer [50mM Tris-HCl,
380 0.1mg/ml BSA, 1mM $MgCl_2$, pH 8]) to the airway using a syringe at a rate of about 10
381 ml/min.

382 To begin the decellularization process, the arterial vasculature was perfused with
383 PBS to facilitate blood clearance and to decontaminate the vasculature (Table 1).
384 Subsequently, the vasculature was perfused with lactated Ringer's solution containing
385 heparin to assist with blood clearance. This step was followed by vascular perfusion with
386 PBS and sodium nitroprusside to dilate the vasculature. To remove blood and residual
387 cell debris, Triton X-100 in PBS was perfused through the vasculature. Triton X-100, a

non-ionic detergent, is expected to solubilize pre-existing cellular debris (i.e. soluble proteins and phospholipids) and to gently permeabilize the plasma and nuclear membranes of the endothelial cells. Membrane permeabilization may occur due to this mild surfactant's preferential dissociation of protein-lipid and lipid-lipid associations [58].

DNA released following Triton X-100 treatment was subsequently cleaved with Benzonase. Benzonase buffer was applied to the vasculature, and was immediately followed by vascular perfusion with Benzonase nuclease in buffer. Afterwards, the lung was temporarily removed from the bioreactor assembly for the manual application of Benzonase buffer to the airways on a sterile instrument tray. The tissue was incubated for 10 minutes with the buffer, after which the airways were manually inflated with Benzonase nuclease in buffer. The tracheal cannula was then capped so that the lung remained inflated for the 2-hour incubation at room temperature. For the duration of the 2-hour incubation, the lung was re-mounted within the bioreactor assembly, such that the tissue remained surrounded by PBS. Following endonuclease treatment, the lung was again removed from the bioreactor apparatus, and the airway was drained passively by removal of the tracheal cannula cap. The lung was then mounted once again within the bioreactor assembly for subsequent rinsing using PBS in order to remove DNA residuals.

Subsequently, lungs were treated with increasing concentrations of sodium deoxycholate (SDC), an anionic detergent, in a solution containing EDTA and, for some steps, NaCl (Table 1). SDC can dissociate protein-protein interactions, thereby fully lysing/disrupting and solubilizing the plasma membrane, nuclear envelope, and intracellular protein networks [59-61]. SDC is also capable of dissolving released and

411 unwound DNA [62-64].

412 We then proceeded with vascular application of a SDC 0.01% solution containing
413 EDTA and NaCl in PBS. A PBS rinse step (after step 7, Table 1) removed residual salt
414 from the prior high-salt step, since SDC solutions have been shown to aggregate in the
415 presence of high concentrations of NaCl. Hence, the solutions containing increasing
416 SDC concentrations were devoid of NaCl in steps 9 and 10 (Table 1) and maintained at
417 pH 8 in order to approach physiological pH while simultaneously reducing the possibility
418 for SDC precipitate formation [58, 65, 66].

419 After the ramping SDC steps, the tissue was rinsed with PBS to remove any
420 remaining detergent micelles. In an effort to disrupt any residual protein-lipid and lipid-
421 lipid interactions that were not eliminated with the initial exposure to 0.0035% Triton X-
422 100, a solution containing 0.5% Triton X-100 and EDTA in PBS was perfused through
423 the vasculature [58]. Given the mild properties of this detergent, it was used at 0.5%,
424 which is the highest concentration used for any detergent in this protocol. A final,
425 thorough rinse of the lung vasculature consisting of PBS concluded the decellularization,
426 and resulted in the generation of a fully decellularized extracellular matrix scaffold (Fig.
427 1 B, E, and F).

428 *Alternative Decellularization Methods*

429 For comparison of the proposed protocol and alternatively published protocols,
430 please refer to Supplememtal Table 2. Upon harvest, lungs were inflated with PBS
431 containing antibiotics (10% penicillin/streptomycin, 4% amphotericin B, 2% gentamicin),
432 cannulated, and perfused with PBS to facilitate blood clearance as per our proposed
433 protocol. All perfusion through the vasculature was done via gravity feed at 22 mm Hg.

Subsequently, porcine lobes were decellularized using one of the following protocols:

Triton X-100/SDC (high concentration): Porcine lobes were decellularized using protocols modified from Bonvillian et al and Price et al [3, 10]. Briefly, on Day 1 the porcine accessory lobes was washed five times (30 ml per installation) via intratracheal inflation with a deionized water solution (DI water, 500 U/mL penicillin, and 500 mg/mL streptomycin). The pulmonary vasculature was then perfused with DI water solution five times (60 ml) to remove any remaining blood. Triton X-100 solution (0.1% Triton X-100, 500 U/mL penicillin, and 500 mg/mL streptomycin) was then instilled into the airway (30 ml) and throughout the vasculature as before (30 ml). The lungs were bathed in the Triton X-100 solution and incubated at 4℃ for 24 hours. On Day 2, the lobe was washed with DI water and subsequently SDC solution (2%) was instilled via the airway (30 ml) and perfused via the vasculature (30 ml). Following SDC installation and perfusion, the lobes underwent exterior bathing and incubation with deoxycholate solution (2% sodium deoxycholate, 100 U/mL penicillin, and 100 mg/mL streptomycin) at 4℃ for 24 hours.

On Day 3, the lobes were removed from deoxycholate solution, washed with DI water solution, and hypertonic saline solution (1M NaCl, 500 U/mL penicillin, and 500 mg/mL streptomycin) was instilled in the airway and subsequently perfused via the vasculature. Following application of the hypertonic saline solution, the lobes were bathed in the NaCl solution at room temperature for 1 hour. The NaCl solution was removed by DI water washes, and a solution of bovine pancreatic DNase (30 mg/mL DNase, 1.3 mM MgSO4, 2 mM CaCl2, 500 U/mL penicillin, and 500 mg/mL streptomycin) was instilled and perfused as before. The lobe was bathed in DNase solution and incubated at room

457 temperature for 1 hour. Following DNase treatment, the lobe was washed five times with
458 PBS solution (PBS without Ca^{2+}/Mg^{2+}, 500 U/mL penicillin, 500 mg/mL streptomycin,
459 and 1.25 mg/mL amphotericin B).

460

461 **SDS:** On Day 1, tissues were decellularized using 0.5% SDS via vascular perfusion (5 L,
462 22 mm Hg). Subsequently to the initial perfusion, the lung was perfused with 0.5% SDS
463 via pulsatile pump for 3 days. Fresh 0.5% SDS was placed into the bioreactor every 24
464 hours. After 3 days of perfusion with SDS, the lung was perfused with DI water for 15
465 minutes, followed by 0.1% Triton for 10 minutes via the vasculature (gravity fed, 22 mm
466 Hg). The lung was then perfused via pulsatile pump for 24 hours with PBS and 1%
467 penicillin/ streptomycin.

468 **Histology and Immunostaining**

469 Several areas of each lung (n=3-5 areas, sampled randomly) were isolated, fixed
470 with 10% formalin for 4 hours at room temperature, stored overnight in 70% ethanol,
471 embedded in paraffin, and sectioned at 5 μm. Tissue slides were stained for hematoxylin
472 and eosin (H&E), Masson's Trichrome staining (Trichrome) for detecting collagen
473 content, Toluidine Blue for detecting GAG quantity, or Verhoeff's Van Gieson (EVG)
474 for detecting elastin. Additionally, tissue slides were stained using 3,3'-
475 diaminobenzidine (DAB) peroxidase substrate kit (Vector Laboratories) for collagen type
476 I (Acris) and fibronectin (Abcam, ab6328) detection.

477 For immunofluorescence, antigen retrieval was performed in 1 mM EDTA, 10 mM
478 Tris and 0.05% Tween 20 buffer at pH 9 for 20 minutes at 75°C and allowed to cool to

room temperature for 20 minutes. After blocking sections with PBS containing 10% FBS and 0.2% Triton X-100 for 45 minutes, primary antibodies were used against laminin (Abcam, ab74164, "2 drops"), collagen IV (Abcam, ab6586, 1:100), and elastin (Abcam, ab21610, 1:50) for 2 hours at room temperature. After washing slides with PBS, corresponding secondary antibodies (Alexafluor 555) were used at 1:500 dilution for 45 minutes. Finally, mounting medium containing 4, 6-diamidino-2-phenylindole (DAPI) was applied. The slides were visualized using a Leica DMI6000 B fluorescence microscope.

Quantitative Matrix Analysis

Collagen assay

Collagen was quantified using a hydroxyproline assay, as previously described [67]. Tissues were digested in 50 U/mL papain (Sigma) overnight at 37°C, and then incubated in 6 N HCl at 110°C for 20 hours, neutralized, oxidized with chloramine-T, and combined with p-dimethylaminobenzaldehyde (Mallinckrodt Baker, Phillipsburg, NJ). Absorbance was measured at a wavelength of 550 nm and a 1:10 w/w ratio of hydroxyproline to collagen was used. Collagen content was normalized to wet tissue weight.

Carbazole assay (total GAGs)

Total GAGS (sulfated and unsulfated) were measured using a carbazole assay [68]. Tissues were digested in 50 U/mL papain (Sigma) overnight at 37°C, tetraborate (Sigma) solution was then added, and the sample incubated for 10 minutes at 100ºC. The sample was then cooled for 15 minutes at room temperature, and carbazole solution (Sigma) was

added. The sample was incubated again for 10 minutes at 100ºC, cooled for 15 minutes at room temperature, and then the absorption of the sample was read at 550 nm and run against a heparin standard (Sigma). Total GAG content was normalized to tissue wet weight.

Sulfated GAG assay

Sulfated glycosaminoglycans, including GAGs such as chondroitin, dermatan, heparan and keratan sulfates, were quantified using the Blyscan GAG assay kit according to manufacturer's instructions. Briefly, after papain digestion, sulfated GAGs were labeled with 1,9-dimethyl-methylene blue dye and absorbance was measured at 650 nm and normalized to tissue wet weight.

DNA Quantification

DNA was isolated and quantified using a Quant-iT PicoGreen dsDNA assay kit (Invitrogen, Eugene, OR), following manufacturer's instructions. Briefly, after papain digest, DNA samples were mixed with the Quant-iT PicoGreen reagent, measured via spectrophotometry at 535 nm with excitation at 485 nm, and DNA content was quantified using a standard curve. DNA content was normalized to wet tissue weight.

Tensile testing

Native and decellularized lung samples were analyzed using an Instron 5848. Nominal 15 x 2 mm (length x width) strips were obtained from tissue samples for testing. Care was taken to analyze tissue from the distal region of the accessory lobe (so as not to include major airways and pleura that could dominate mechanical analysis). Tissue

524 thickness of each sample was determined by a series of measurements at four different
525 points using a Mitutoyo digital micrometer. Specimens were glued to 1 mm sections of
526 sand paper at each end of the tissue slices, and each end was affixed to grips. Tissues
527 were then pretared to 0.01 N, cyclically preconditioned for 3 cycles to 15% strain, and
528 pulled until failure at a strain rate of 1%/sec. The axial force was measured with a 10 N
529 load cell, and elongation assessed by cross-head displacement. Tissues were kept
530 hydrated with PBS before and during the mechanical conditioning. Using tissue
531 dimensions, engineering stress and strain were calculated from force and distance from
532 the slope at the linear regions of the curve using the equations 2.1-2.2:

533 $\sigma = \frac{F}{A_0}$ where σ is engineering stress, F = Force, and A_0 = initial area (2.1)

534 $\varepsilon = \frac{l_f - l_o}{l_o}$ where ε = engineering strain, l_f= final length, l_0= initial length. (2.2)

535 The Young's Modulus (E) for the tissue was determined by dividing the engineering
536 stress,σ, by the engineering strain, ε, at low and high levels of deformation.

537

538 **Western blotting**

539 For total protein analysis, tissue was immunoblotted as described previously [69].
540 Briefly, tissues were frozen in liquid nitrogen, and then ground into a fine powder with a
541 mortar and pestle. Tissue powder was then resuspended in RIPA buffer supplemented
542 with protease inhibitor cocktail (Complete Mini, Roche, Bath, UK) for 1 hour on ice.
543 Tissue solutions were homogenized for 30 seconds and subsequently centrifuged at
544 10,000 rpm for 10 minutes. The supernatant was removed and protein concentration was

545 determined from native cell lysates using a bicinchoninic acid protein assay (Thermo
546 Fisher Scientific, Lafayette, CO) with bovine serum albumin as a standard. Lysates were
547 denatured, and equal amounts of protein (10 μg for vimentin) were subjected to SDS-
548 PAGE followed by immunoblotting as described previously [69]. We used HRP-
549 conjugated secondary goat anti-mouse and goat anti-rabbit antibodies (Invitrogen)
550 detected by enhanced chemiluminescence.
551

552 **Statistics**

553 Data are presented as the mean with standard error bars representing the standard
554 deviation. Data were analyzed by Student's t-test for significance and considered
555 significantly different if $p < 0.05$.

556

557 **Acknowledgements and support**

558 The authors would like to thank Deborah Caruso, Meghan Connolly, Lyn Patrylak, and
559 Morgan Oexner with the Veterinary Care Services at Yale for their invaluable technical
560 assistance during tissue procurement, Peter Smith for his logistical assistance, Daryl
561 Smith for his technical assistance with the construction of the lobe bioreactor, and Joseph
562 Latella at Latella's piggery for his generous donation of pig lungs in initial
563 decellularization studies. This work was supported by a grant from United Therapeutics,
564 Inc, and by and NIH U01 HL111016-01 (both to LEN). L.E.N. has a financial interest in
565 Humacyte, Inc, a regenerative medicine company. Humacyte did not fund these studies,
566 and Humacyte did not affect the design, interpretation, or reporting of any of the
567 experiments herein.

[1] Mannino DM, Homa DM, Akinbami LJ, Ford ES, Redd SC. Chronic obstructive pulmonary disease surveillance--United States, 1971-2000. Respir Care. 2002;47:1184-99.
[2] Wilkes DS. A breath of fresh air for lung transplant recipients. Sci Transl Med. 2009;1:4ps5.
[3] Bonvillain RW, Danchuk S, Sullivan DE, Betancourt AM, Semon JA, Eagle ME, et al. A nonhuman primate model of lung regeneration: detergent-mediated decellularization and initial in vitro recellularization with mesenchymal stem cells. Tissue Eng Part A. 2012;18:2437-52.
[4] Petersen TH, Calle EA, Zhao L, Lee EJ, Gui L, Raredon MB, et al. Tissue-engineered lungs for in vivo implantation. Science. 2010;329:538-41.
[5] Calle EA, Petersen TH, Niklason LE. Procedure for lung engineering. J Vis Exp. 2011.
[6] Booth AJ, Hadley R, Cornett AM, Dreffs AA, Matthes SA, Tsui JL, et al. Acellular normal and fibrotic human lung matrices as a culture system for in vitro investigation. Am J Respir Crit Care Med. 2012;186:866-76.
[7] Song JJ, Kim SS, Liu Z, Madsen JC, Mathisen DJ, Vacanti JP, et al. Enhanced in vivo function of bioartificial lungs in rats. Ann Thorac Surg. 2011;92:998-1005; discussion -6.
[8] Song JJ, Ott HC. Bioartificial lung engineering. Am J Transplant. 2012;12:283-8.
[9] Bonenfant NR, Sokocevic D, Wagner DE, Borg ZD, Lathrop MJ, Lam YW, et al. The effects of storage and sterilization on de-cellularized and re-cellularized whole lung. Biomaterials. 2013;34:3231-45.
[10] Price AP, England KA, Matson AM, Blazar BR, Panoskaltsis-Mortari A. Development of a Decellularized Lung Bioreactor System for Bioengineering the Lung: The Matrix Reloaded. Tissue Eng Part A. 2010;16:2581-91.
[11] Gilpin SE, Ott HC. Using nature's platform to engineer bio-artificial lungs. Annals of the American Thoracic Society. 2015;12 Suppl 1:S45-9.
[12] Gilpin SE, Ren X, Okamoto T, Guyette JP, Mou H, Rajagopal J, et al. Enhanced lung epithelial specification of human induced pluripotent stem cells on decellularized lung matrix. Ann Thorac Surg. 2014;98:1721-9; discussion 9.
[13] O'Neill JD, Anfang R, Anandappa A, Costa J, Javidfar J, Wobma HM, et al. Decellularization of human and porcine lung tissues for pulmonary tissue engineering. Ann Thorac Surg. 2013;96:1046-55; discussion 55-6.
[14] Wagner DE, Bonenfant NR, Parsons CS, Sokocevic D, Brooks EM, Borg ZD, et al. Comparative decellularization and recellularization of normal versus emphysematous human lungs. Biomaterials. 2014;35:3281-97.
[15] Gilpin SE, Guyette JP, Gonzalez G, Ren X, Asara JM, Mathisen DJ, et al. Perfusion decellularization of human and porcine lungs: Bringing the matrix to clinical scale. J Heart Lung Transplant. 2014.
[16] Nichols JE, Niles J, Riddle M, Vargas G, Schilagard T, Ma L, et al. Production and assessment of decellularized pig and human lung scaffolds. Tissue Eng Part A. 2013;19:2045-62.

[17] Price AP, Godin LM, Domek A, Cotter T, D'Cunha J, Taylor DA, et al. Automated decellularization of intact, human-sized lungs for tissue engineering. Tissue Eng Part C Methods. 2015;21:94-103.
[18] Brown BN, Badylak SF. Extracellular matrix as an inductive scaffold for functional tissue reconstruction. Transl Res. 2013.
[19] Crapo PM, Medberry CJ, Reing JE, Tottey S, van der Merwe Y, Jones KE, et al. Biologic scaffolds composed of central nervous system extracellular matrix. Biomaterials. 2012;33:3539-47.
[20] Reing JE, Brown BN, Daly KA, Freund JM, Gilbert TW, Hsiong SX, et al. The effects of processing methods upon mechanical and biologic properties of porcine dermal extracellular matrix scaffolds. Biomaterials. 2010;31:8626-33.
[21] Zheng MH, Chen J, Kirilak Y, Willers C, Xu J, Wood D. Porcine small intestine submucosa (SIS) is not an acellular collagenous matrix and contains porcine DNA: possible implications in human implantation. J Biomed Mater Res B Appl Biomater. 2005;73:61-7.
[22] Crapo PM, Gilbert TW, Badylak SF. An overview of tissue and whole organ decellularization processes. Biomaterials. 2012;32:3233-43.
[23] Lotze MT, Zeh HJ, Rubartelli A, Sparvero LJ, Amoscato AA, Washburn NR, et al. The grateful dead: damage-associated molecular pattern molecules and reduction/oxidation regulate immunity. Immunol Rev. 2007;220:60-81.
[24] Lotze MT, Deisseroth A, Rubartelli A. Damage associated molecular pattern molecules. Clin Immunol. 2007;124:1-4.
[25] Gilbert TW, Sellaro TL, Badylak SF. Decellularization of tissues and organs. Biomaterials. 2006;27:3675-83.
[26] Neame SJ, Uff CR, Sheikh H, Wheatley SC, Isacke CM. CD44 exhibits a cell type dependent interaction with triton X-100 insoluble, lipid rich, plasma membrane domains. J Cell Sci. 1995;108 (Pt 9):3127-35.
[27] Schuck S, Honsho M, Ekroos K, Shevchenko A, Simons K. Resistance of cell membranes to different detergents. Proc Natl Acad Sci U S A. 2003;100:5795-800.
[28] Faulk DM, Carruthers CA, Warner HJ, Kramer CR, Reing JE, Zhang L, et al. The effect of detergents on the basement membrane complex of a biologic scaffold material. Acta Biomater. 2014;10:183-93.
[29] Tsukahara H, Noiri E, Jiang MZ, Hiraoka M, Mayumi M. Role of nitric oxide in human pulmonary microvascular endothelial cell adhesion. Life Sci. 2000;67:1-11.
[30] Petersen TH, Calle EA, Colehour MB, Niklason LE. Matrix composition and mechanics of decellularized lung scaffolds. Cells Tissues Organs. 2012;195:222-31.
[31] Papakonstantinou E, Karakiulakis G. The 'sweet' and 'bitter' involvement of glycosaminoglycans in lung diseases: pharmacotherapeutic relevance. Br J Pharmacol. 2009;157:1111-27.
[32] Suki B. Assessing the functional mechanical properties of bioengineered organs with emphasis on the lung. J Cell Physiol. 2014;229:1134-40.
[33] Suki B, Stamenovic D, Hubmayr R. Lung parenchymal mechanics. Compr Physiol. 2011;1:1317-51.
[34] Balestrini JL, Skorinko JK, Hera A, Gaudette GR, Billiar KL. Applying controlled non-uniform deformation for in vitro studies of cell mechanobiology. Biomech Model Mechanobiol. 2010;9:329-44.

[35] Breen EC. Mechanical strain increases type I collagen expression in pulmonary fibroblasts in vitro. J Appl Physiol. 2000;88:203-9.
[36] Sugihara T, Martin CJ, Hildebrandt J. Length-tension properties of alveolar wall in man. J Appl Physiol. 1971;30:874-8.
[37] Keane TJ, Londono R, Turner NJ, Badylak SF. Consequences of ineffective decellularization of biologic scaffolds on the host response. Biomaterials.33:1771-81.
[38] Sokocevic D, Bonenfant NR, Wagner DE, Borg ZD, Lathrop MJ, Lam YW, et al. The effect of age and emphysematous and fibrotic injury on the re-cellularization of de-cellularized lungs. Biomaterials. 2013;34:3256-69.
[39] Ott HC, Clippinger B, Conrad C, Schuetz C, Pomerantseva I, Ikonomou L, et al. Regeneration and orthotopic transplantation of a bioartificial lung. Nat Med. 2010;16:927-33.
[40] Tsuchiya T, Balestrini JL, Mendez J, Calle EA, Zhao L, Niklason LE. Influence of pH on Extracellular Matrix Preservation During Lung Decellularization. Tissue Eng Part C Methods. 2014.
[41] Gui L, Chan SA, Breuer CK, Niklason LE. Novel utilization of serum in tissue decellularization. Tissue Eng Part C Methods. 2010;16:173-84.
[42] Whitelock JM, Iozzo RV. Heparan sulfate: a complex polymer charged with biological activity. Chem Rev. 2005;105:2745-64.
[43] Tsuchiya T, Balestrini JL, Mendez JJ, Calle EA, Zhao L, Niklason L. Influence of pH on Extracellular Matrix Preservation During Lung Decellularization. Tissue Eng Part C Methods. 2014.
[44] Brown BN, Freund JM, Han L, Rubin JP, Reing JE, Jeffries EM, et al. Comparison of three methods for the derivation of a biologic scaffold composed of adipose tissue extracellular matrix. Tissue Eng Part C Methods. 2011;17:411-21.
[45] Gilbert TW, Wognum S, Joyce EM, Freytes DO, Sacks MS, Badylak SF. Collagen fiber alignment and biaxial mechanical behavior of porcine urinary bladder derived extracellular matrix. Biomaterials. 2008;29:4775-82.
[46] Gorschewsky O, Puetz A, Riechert K, Klakow A, Becker R. Quantitative analysis of biochemical characteristics of bone-patellar tendon-bone allografts. Biomed Mater Eng. 2005;15:403-11.
[47] Chen X, Stewart PS. Biofilm removal caused by chemical treatments. Water Research. 2000;34:4229-33.
[48] Jeong EK, Bae JE, Kim IS. Inactivation of influenza A virus H1N1 by disinfection process. Am J Infect Control. 2010;38:354-60.
[49] Komatsuzawa H, Sugai M, Shirai C, Suzuki J, Hiramatsu K, Suginaka H. Triton X-100 alters the resistance level of methicillin-resistant Staphylococcus aureus to oxacillin. FEMS Microbiol Lett. 1995;134:209-12.
[50] Lomas RJ, Jennings LM, Fisher J, Kearney JN. Effects of a peracetic acid disinfection protocol on the biocompatibility and biomechanical properties of human patellar tendon allografts. Cell Tissue Bank. 2004;5:149-60.
[51] Hodde J, Janis A, Ernst D, Zopf D, Sherman D, Johnson C. Effects of sterilization on an extracellular matrix scaffold: part I. Composition and matrix architecture. J Mater Sci Mater Med. 2007;18:537-43.
[52] Gefen A, Elad D, Shiner RJ. Analysis of stress distribution in the alveolar septa of normal and simulated emphysematic lungs. J Biomech. 1999;32:891-7.

[53] Lovekamp JJ, Simionescu DT, Mercuri JJ, Zubiate B, Sacks MS, Vyavahare NR. Stability and function of glycosaminoglycans in porcine bioprosthetic heart valves. Biomaterials. 2006;27:1507-18.
[54] Stahl WR. Scaling of respiratory variables in mammals. J Appl Physiol. 1967;22:453-60.
[55] Tillery SI, Lehnert BE. Age-bodyweight relationships to lung growth in the F344 rat as indexed by lung weight measurements. Lab Anim. 1986;20:189-94.
[56] Hirsh J, Anand SS, Halperin JL, Fuster V, American Heart A. Guide to anticoagulant therapy: Heparin : a statement for healthcare professionals from the American Heart Association. Circulation. 2001;103:2994-3018.
[57] Petersen TH, Calle EA, Colehour MB, Niklason LE. Bioreactor for the long-term culture of lung tissue. Cell Transplant. 2011;20:1117-26.
[58] Seddon AM, Curnow P, Booth PJ. Membrane proteins, lipids and detergents: not just a soap opera. Biochim Biophys Acta. 2004;1666:105-17.
[59] Kirschner RH, Rusli M, Martin TE. Characterization of the nuclear envelope, pore complexes, and dense lamina of mouse liver nuclei by high resolution scanning electron microscopy. J Cell Biol. 1977;72:118-32.
[60] Rabinovitz I, Mercurio AM. The integrin alpha6beta4 functions in carcinoma cell migration on laminin-1 by mediating the formation and stabilization of actin-containing motility structures. J Cell Biol. 1997;139:1873-84.
[61] Stevenson BR, Goodenough DA. Zonulae occludentes in junctional complex-enriched fractions from mouse liver: preliminary morphological and biochemical characterization. J Cell Biol. 1984;98:1209-21.
[62] Powolny A, Xu J, Loo G. Deoxycholate induces DNA damage and apoptosis in human colon epithelial cells expressing either mutant or wild-type p53. Int J Biochem Cell Biol. 2001;33:193-203.
[63] Jolly AJ, Wild CP, Hardie LJ. Acid and bile salts induce DNA damage in human oesophageal cell lines. Mutagenesis. 2004;19:319-24.
[64] Crowley CL, Payne CM, Bernstein H, Bernstein C, Roe D. The NAD+ precursors, nicotinic acid and nicotinamide protect cells against apoptosis induced by a multiple stress inducer, deoxycholate. Cell Death Differ. 2000;7:314-26.
[65] Murata Y, Sugihara G, Fukushima K, Tanaka M, Matsushita K. Study of the micelle formation of sodium deoxycholate. Concentration dependence of carbon-13 nuclear magnetic resonance chemical shift. J Phys Chem. 1982;Nov;86:4690-4.
[66] Coello A, Meijide F, Rodriguez Nunez E, Vazquez Tato J. Aggregation behavior of sodium cholate in aquestion solution. J Phys Chem 1993;97:10186-91.
[67] Woessner JF, Boucek RJ. Connective Tissue Development in Subcutaneously Implanted Polyvinyl Sponge. Archives of Biochemistry and Biophysics. 1961;93:85-94.
[68] Warda M, Gouda EM, Toida T, Chi L, Linhardt RJ. Isolation and characterization of raw heparin from dromedary intestine: evaluation of a new source of pharmaceutical heparin. Comp Biochem Physiol C Toxicol Pharmacol. 2003;136:357-65.
[69] Balestrini JL, Chaudhry S, Sarrazy V, Koehler A, Hinz B. The mechanical memory of lung myofibroblasts. Integr Biol (Camb). 2012;4:410-21.

Table and Figure Legends

Table 1: Concentrations, volumes, temperatures and pHs of solutions utilized in the decellularization protocol. V = Vasculature, A = Airways, * = 10 minute exposure time, ǂ = 2 hour exposure time, Δ = Syringe depression rate = 10 ml/min.

Figure 1. Decellularization protocol yields acellular scaffolds from whole lungs and individual lobes. Marcroscopic images of A) whole pig lungs and B) individual lobes before and after decellularization. H&E stained sections of native and decellularized tissue from intact whole lungs (C and E) or individual lobes (D and F). Scale bar = 100 μm

Figure 2. Characterization of decellularized lung matrix. Native and decellularized lung tissue stained with Masson's Trichrome shows maintenance of tissue architecture (A and F, collagen in blue) and removal of cell debris and blood (A and F, cells in red). Collagen type I fibers are preserved (B and G, in brown), as are elastin fibers (verhoeff's van gieson (EVG) stain, C and H, in dark purple), fibronectin (D and I, in brown), and GAGs (D and J, in blue) throughout the tissue after decellularization. Scale bar = 100 μm applies to all panels.

Figure 3. Decellularized accessory lobes maintain key matrix proteins. Immunofluorescence for (A and E) laminin, (B and F) collagen IV, (D and H) elastin (EVG) show presence of structural and adhesive matrix proteins without any intact nuclei

769 (shown by DAPI stain in blue) after decellularization. Scale bar = 100 μm applies to all
770 panels.
771
772 **Figure 4. Quantifying decellularization efficiency of proposed protocol.**
773 Quantification of A) total GAGs B) sulfated GAGs and C) unsulfated GAGs in native
774 (n=12) and decellularized tissue (n=15) demonstrate a depletion of sulfated GAGs and
775 retention of unsulfated GAGs. D) Collagen content of native (n = 6) and decellularized (n
776 = 12) indicate the retention of collagen post decellularization. E) DNA mg/mg of native
777 (n=5) and decellularized tissue (n=15) indicate the absence of nuclear material post
778 decellularization. F) Immunoblotting for vimentin demonstrate the absence of
779 cytoskeletal proteins in decellularized matrix. All quantitiative measurements were
780 normalized to tissue wet weight. Error bars show mean ± standard deviation, and *
781 indicates significance at $p \leq 0.05$.
782
783 **Figure 5. Characterization of tissue architecture, DNA content, sulfated**
784 **glycosaminoglycans, and mechanical properties of decellularized lung tissue.** A)
785 H&E stained sections of native lung or decellularized tissue using three methods.
786 Quantification of B) DNA and C) sulfated GAGs in native and decellularized tissue using
787 "Current Method" (n=15), Triton X-100/SDC (n=5), or SDS (n=5). All measurements
788 were normalized to tissue wet weight. D) Stress-strain curves of native and decellularized
789 lung tissue (n=9 for all groups). E) Biochemical and mechanical composition of tissues in
790 native and decellularized conditions. Error bars show mean ± standard deviation, and *
791 indicates significance at $p \leq 0.05$. Scale bar = 100 μm.

Figure 6. Recellularization of lung tissue slices. H&E stained images of recellularized tissue. Acellular tissues were produced using three decellularization methods, recellularized using A549s a concentration of 500,000 cells/slice, and subsequently cultured for 3 days. Acellular tissues procured using the Triton/SDS I method enabled homogeneous epithelial cell engraftment in both the large airways and the alveolar regions of the tissue. Acellular tissues procured via the Triton/SDC II protocol did not promote cell engraftment throughout the tissue, rather cells adhered to the perimeter of the tissue only demonstrating preference to the tissue culture plastic over the acellular tissue. Tissues produced using the SDS protocol engrafted throughout the tissue, although the tissue was much more sparse than the Triton X/SDC I protocol. Scale bar = 50 μm

Supplemental Table 1: **Components of the bioreactor**. Included are specifications of each bioreactor component.

Supplemental Table 2: Comparison of previously published decellularization methods.

Supplemental Figure 1: Bioreactor Design and Assembly. A) The lung or lobe is cannulated via the airways (trachea or bronchiole) and the vasculature (PA or artery) for decellularization. B) The decellularization chamber consists of a cylindrical glass reservoir fitted with a threaded plastic gasket and cap equipped with air filters, a syringe

814 port, and perfusion line. The container is perfused via a gravity-driven system and
815 maintained at a constant pressure head of 22 mm Hg.
816
817 **Supplemental Figure 2: Flow diagram of decellularization.** Schematic of proposed
818 decellularization procedure. Total time for the procedure is 16 hours and 35 minutes.
819
820
821
822
823

Table 1.
Concentrations, volumes, temperatures and pHs of solutions utilized in the decellularization protocol.

Step	***Reagents***	***Volume/weight tissue, (ml/g)***	***pH***	***Temp,°C***	***Route of Admin., V or A***
1a	PBS (w/ Ca^{++} & Mg^{++}) + Antibiotics	3	7.4	4	A
1b	PBS (w/ Ca^{++} & Mg^{++}) + Antibiotics	100	7.4	4	V
2	Lactated Ringer's Solution + Heparin, *100U/ml*	50	7.4	4	V
3	PBS (w/ Ca^{++} & Mg^{++}) + Sodium nitroprisside	50	7.4	4	V
4	Triton X-100, *0.0035%* in PBS (w/ Ca^{++} & Mg^{++})	50	7.4	4	V
5a.1	Benzonase Nuclease Buffer	50	8	37	V
5a.2	Benzonase Nuclease, *40U*	50	8	37	V
5b.1	Benzonase Nuclease Buffer $^{\Delta}$*	3	8	37	A
5b.2	Benzonase Nuclease, *40U* $^{\Delta ǂ}$	3	8	37	A
6	PBS (w/ Ca^{++} & Mg^{++}) + Antibiotics	25	7.4	25	V
7	Sodium Deoxycholate, *0.01%* + EDTA, *5mM* + NaCl, *1M* in PBS	100	8	25	V
8	PBS (w/ Ca^{++} & Mg^{++}) + Antibiotics	25	7.4	25	V
9	Sodium Deoxycholate, *0.05%* + EDTA, *5mM* in PBS	100	8	25	V
10	Sodium Deoxycholate, *0.1%* + EDTA, *5mM* in PBS	100	8	25	V
11	PBS (w/ Ca^{++} & Mg^{++}) + Antibiotics	75	7.4	25	V
12	Triton, *0.5%* + EDTA, *5mM* in PBS	12.5	7.4	25	V
13	PBS (w/ Ca^{++} & Mg^{++}) + Antibiotics	500	7.4	25	V

V = Vasculature, A = Airways, * = 10 minute exposure time, ǂ = 2 hour exposure time,
Δ = Syringe depression rate = 10 ml/min.

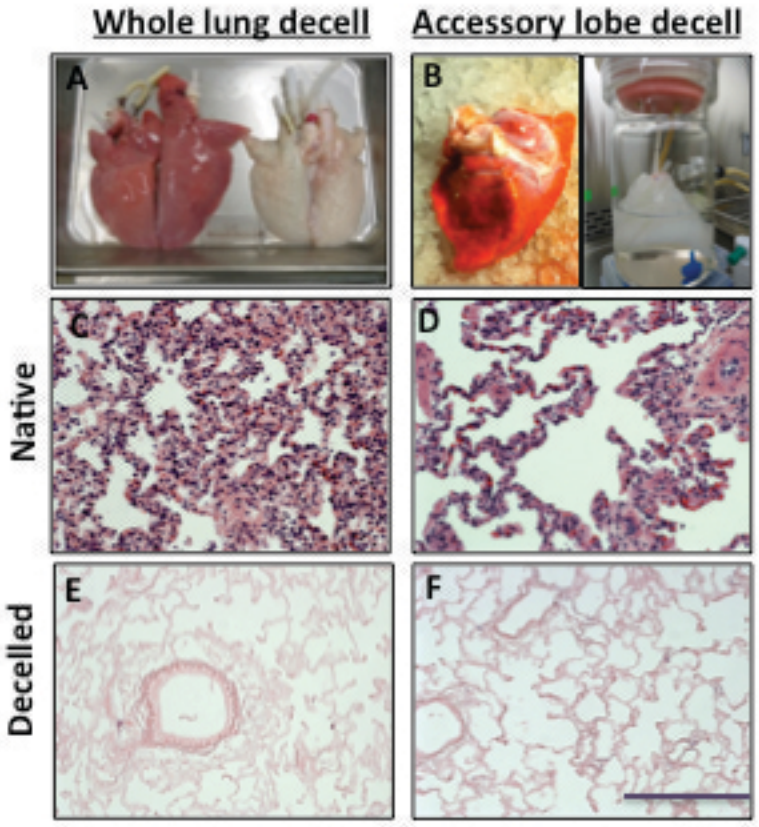

Figure 1. Decellularization protocol yields acellular scaffolds from whole lungs and individual lobes. Macroscopic images of A) whole pig lungs and B) individual lobes before and after decellularization. H&E stained sections of native and decellularized tissue from intact whole lungs (C, E) or individual lobes (D, F). Scale bar = 100 μm.

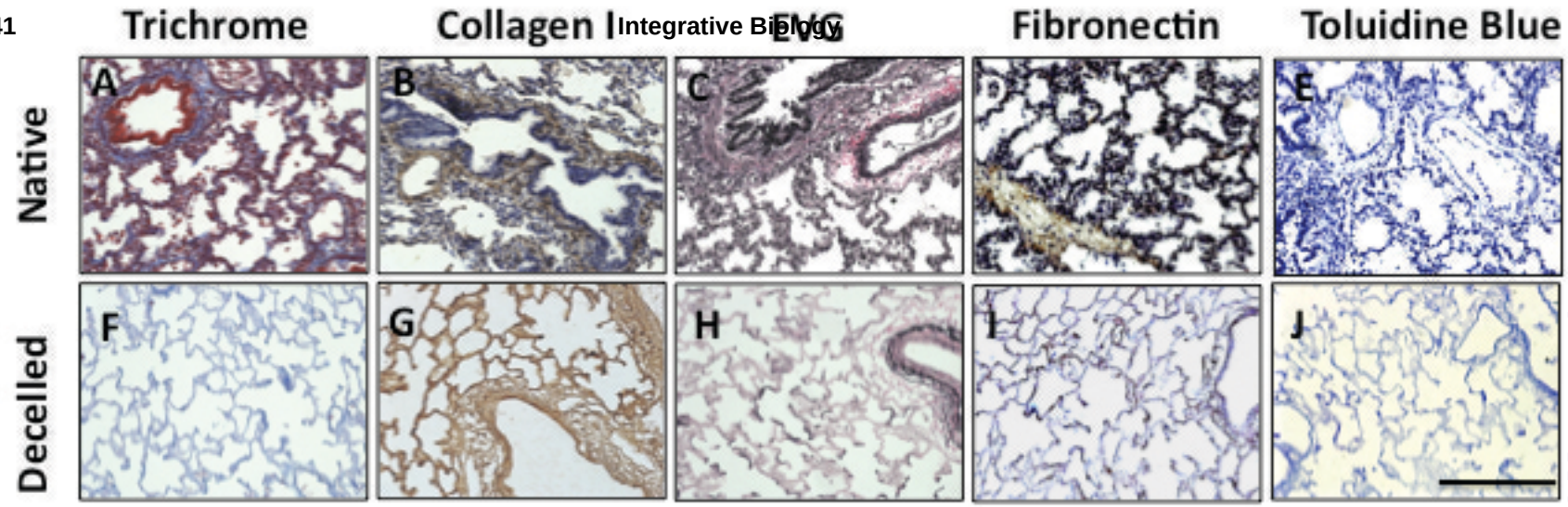

Figure 2. Characterization of decellularized lung matrix. Native and decellularized lung tissue stained with Masson's Trichrome shows maintenance of tissue architecture (A and F, collagen in blue) and removal of cell debris and blood (A and F, cells in red). Collagen type I fibers are preserved (B and G, in brown), as are elastin fibers (C and H, in dark purple), fibronection (D and I, in brown), and GAGs (D and J, in blue) throughout the tissue after decellularization. Scale bar = 100 μm applies to all panels.

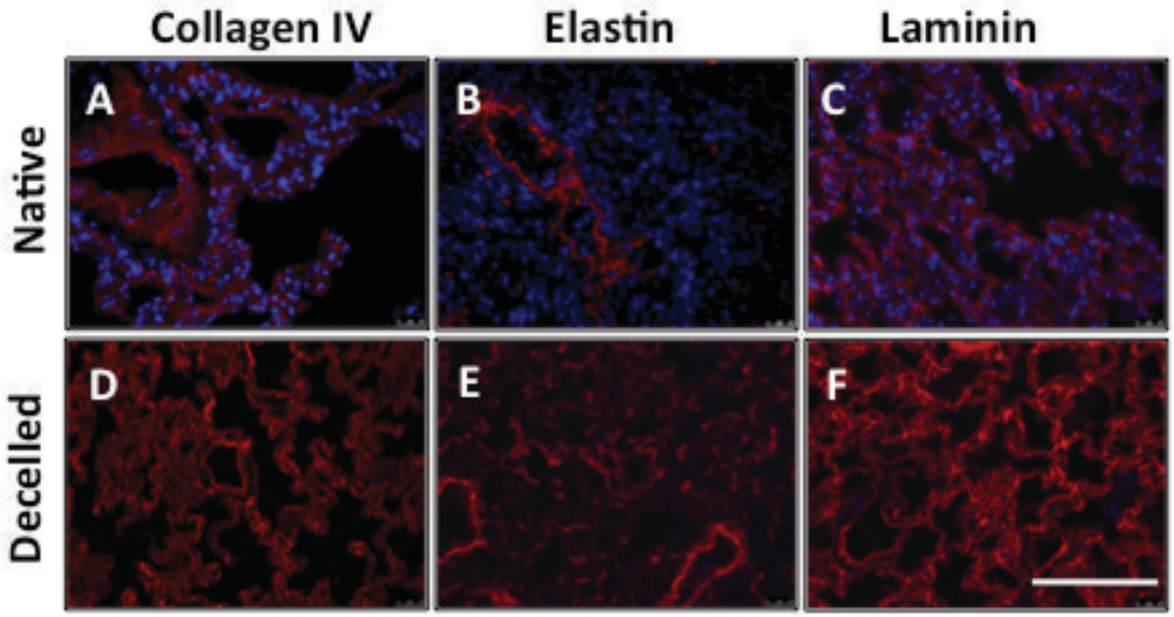

Figure 3. Decellularized accessory lobes maintain key matrix proteins. Immunofluorescence for (A,E) laminin, (B,F) collagen IV, (D,H) elastin show presence of structural and adhesive matrix proteins without any intact nuclei (shown by DAPI stain in blue) after decellularization. Scale bar = 100 μm applies to all panels.

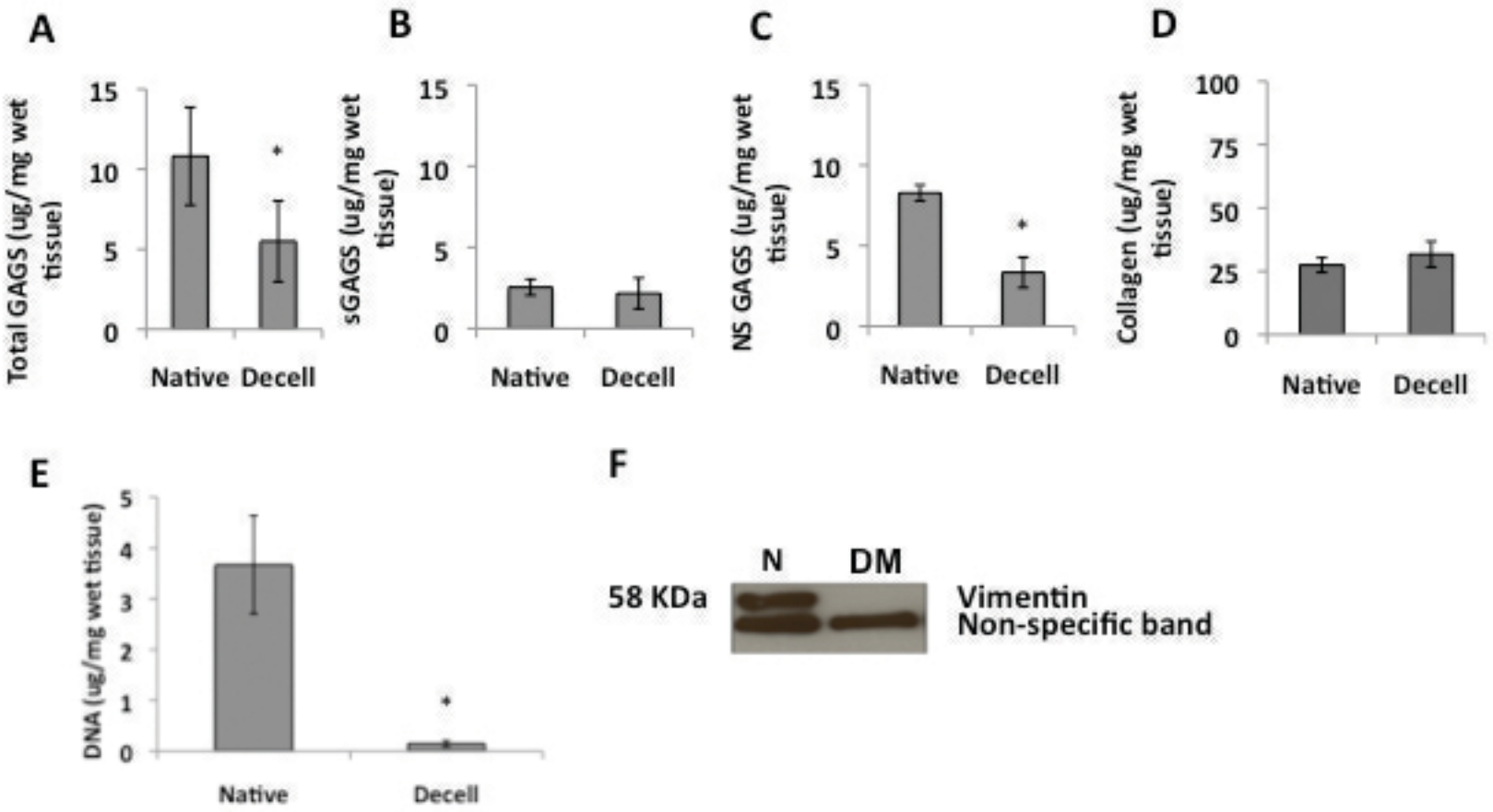

Figure 4. Quantifying decelluarization efficiency. Quantification of A) total GAGs B) sulfated GAGs and C) unsulfated GAGs in native (n=12) and decellularized tissue (n=15) demonstrate a retention of sulfated GAGs and depletion of unsulfated GAGs. D) Collagen content of native (n = 6) and decellularized (n = 12) indicate the retention of collagen post decellularization. E) DNA μg/mg of native (n=5) and decelled tissue (n=15) indicate the absence of nuclear material post decellularization. F) Immunoblotting for vimentin demonstrate the absence of cytoskeletal proteins in decellularized matrix. Error bars show mean ± standard deviation, and * indicates significance at $p \leq 0.05$.

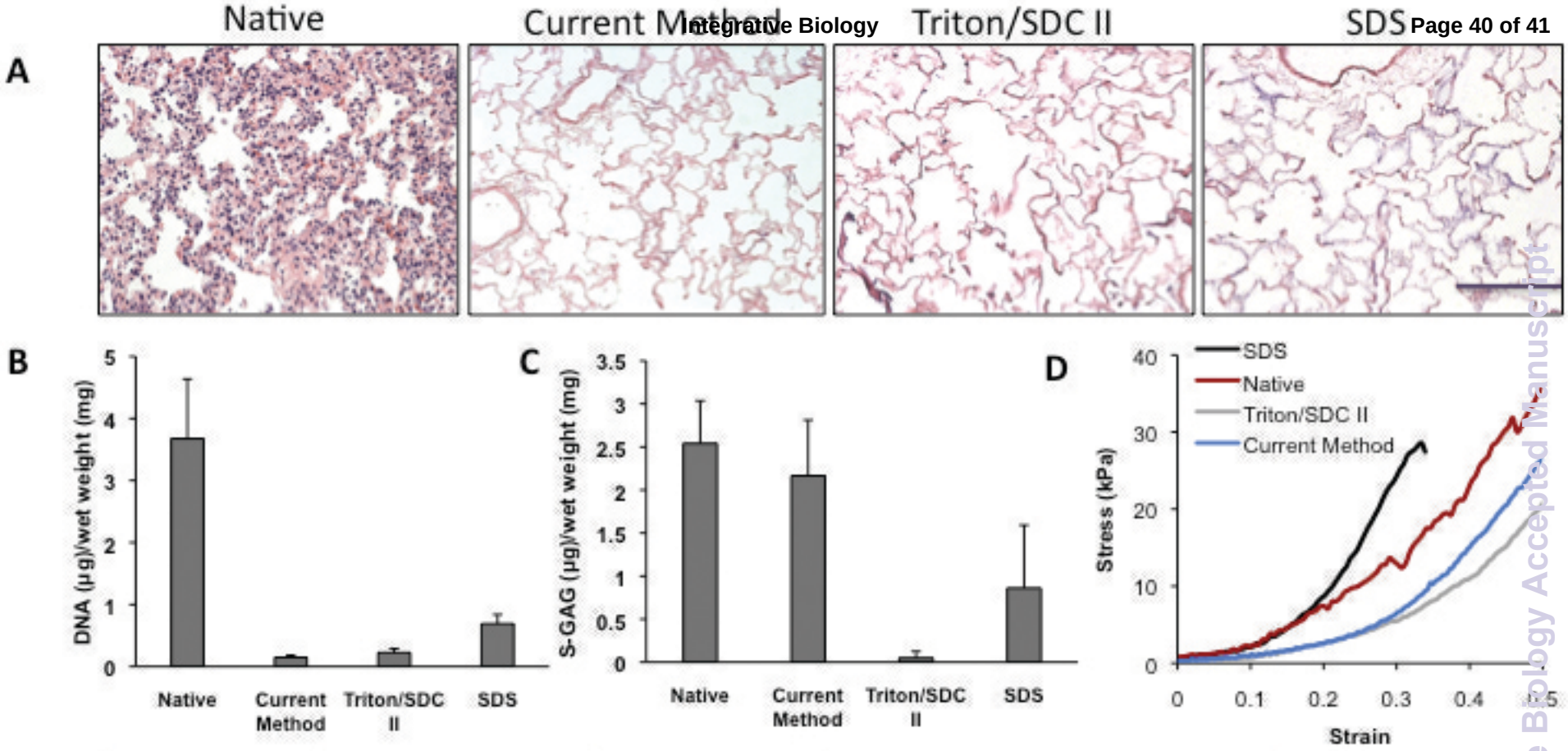

E

	DNA (µg/ mg tissue)	GAG (µg/ mg tissue)	Young's Moduli (kPa) 5%	30%
Native	3.68 ± 0.96	2.54 ± 0.50	8.52 ± 4.12	77.71 ± 10.49
Current Method	0.15 ± 0.03 *	2.16 ± 0.65	6.81 ± 2.41	67.36 ± 7.60
Triton/SDC II	0.23 ± 0.06 *	0.05 ± 0.08 *	5.37 ± 1.15	54.29 ± 10.40 *
SDS	0.69 ± 0.15 *	0.86 ± 0.73 *	9.28 ± 2.37	143.54 ± 28.53 *

Figure 5. Characterization of tissue architecture, DNA content, sulfated glycosaminoglycans and mechanical properties of decellularized lung tissue. A) H&E stained sections of native lung or tissue decellularized using three methods. Quantification of B) DNA and C) sulfated GAGs in native and tissue decellularized using Triton X-100/SDC I (n=15), Triton/SDC II (n=5) or SDS (n=5). D) Stress strain curves of native and decellularized lung tissue (n=9 for all groups). E) Biochemical and mechanical composition of tissues in native and decellularized conditions.

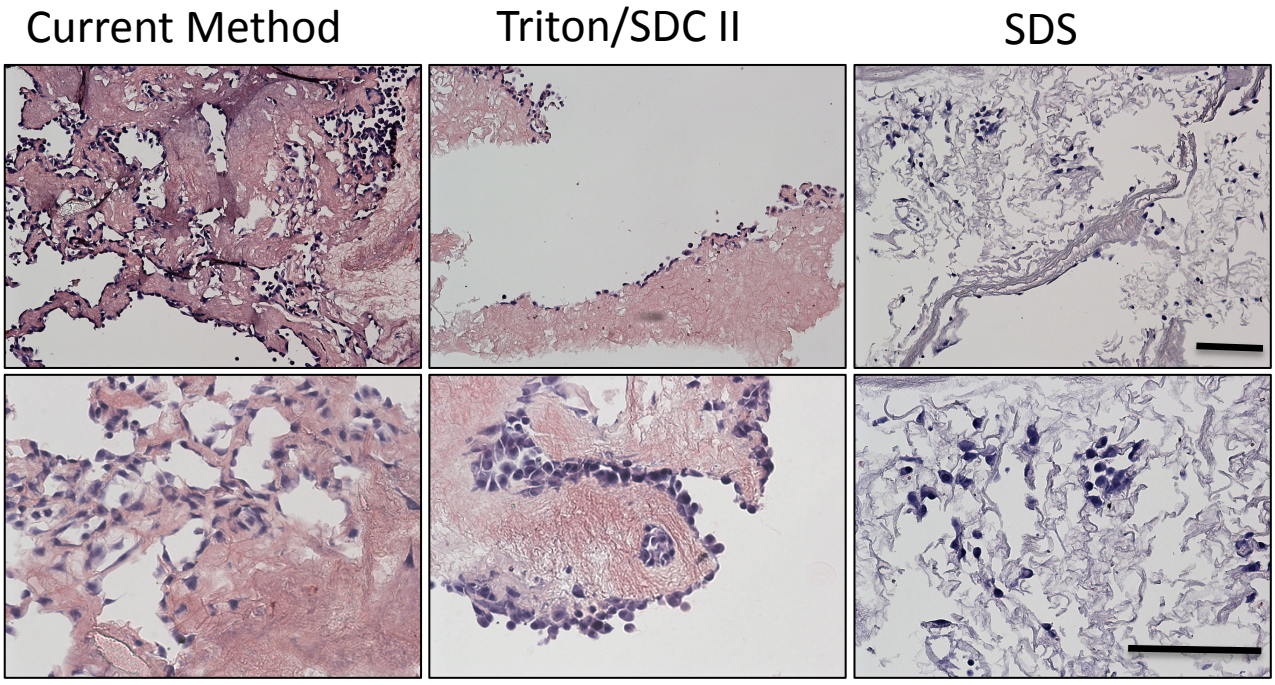

Figure 6. Recellularization of lung tissue slices. H&E stained images of recellularized tissue. Acellular tissues were produced using three decellularization methods, recellularized using A549s a concentration of 500,000 cells/slice, and subsequently cultured for 3 days. Acellular tissues procured using the Triton/SDS I method enabled homogeneous epithelial cell engraftment in both the large airways and the alveolar regions of the tissue. Acellular tissues procured via the Triton/SDC II protocol did not promote cell engraftment throughout the tissue, rather cells adhered to the perimeter of the tissue only demonstrating preference to the tissue culture plastic over the acellular tissue. Tissues produced using the SDS protocol engrafted throughout the tissue, although the tissue was much more sparse than the Triton X/SDC I protocol. Scale bar = 50 μm